JOURNAL OF MATERIALS SCIENCE 22 (1987) 4190–4198

Review
Exfoliation of graphite

D. D. L. CHUNG
Department of Mechanical and Aerospace Engineering, State University of New York, Buffalo, New York 14260, USA

The exfoliation of graphite is a phase transition involving the vaporization of the intercalate in the graphite. Exfoliated graphite is an expanded graphite with a low density. This paper reviews the process of the exfoliation of graphite and the exfoliated graphite material. It surveys the applications of exfoliated graphite, covers both reversible and irreversible exfoliation and reviews the methods and mechanism of exfoliation. Other topics include the structure and properties of exfoliated graphite, graphite foils, exfoliated carbon fibres and composites.

1. Introduction

The exfoliation of graphite is a process in which graphite expands by up to hundreds of times along the c axis, resulting in a puffed-up material with a low density and a high temperature resistance. Moreover, the compression of exfoliated graphite results in a material of high lubricity and flexibility. Exfoliated graphite can also serve as a filler in composites. Even carbon fibres themselves may be exfoliated under appropriate conditions. This paper reviews the technology and science of the exfoliation process and the exfoliated graphite material.

2. Applications of exfoliated graphite

2.1. Gaskets, seals and packings

The compression of exfoliated graphite particles in the absence of a binder results in a flexible sheet material which is useful for high-temperature gaskets [1–4]. By compressing exfoliated graphite together with a reinforcing metal layer, a gasket capable of withstanding an internal pressure of 34 500 kN m^{-2} can be formed [5]. To provide packings which prevent the seizing of shaft materials, one can vapour-deposit a metal with a low melting point, such as lead, on the inner surface on an exfoliated graphite ring [6]. In addition, composites of exfoliated graphite and furan resins serve as gaskets with low adhesion to pressing plates [7].

A refractory sealing material can be formed by adding a binder and exfoliated graphite to a refractory aggregate and heating it to yield a non-porous sealing layer. The sealant is especially useful for preventing gas leakage from blast furnaces and other refractory pressure vessels [8].

A packing material exhibiting high sealing strength under repeated heating cycles is a composite of exfoliated graphite, fibre fillers and a rubber binder. Nitrogen gas leakage is < 0.01 cm^3 min^{-1} initially and ~ 0.01 cm^3 min^{-1} after 3 h of heating cycles between room temperature and 180° C under 60 kg cm nut torque and 10 kg cm^{-2} nitrogen pressure, compared with < 0.01 cm^3 min^{-1} and ~ 0.1 cm^3 min^{-1}, respectively, when a packing material contains natural graphite instead of exfoliated graphite [9].

2.2. Fire extinguisher agents

Exfoliated graphite is commercially available as a fire extinguisher agent which is valuable for the extinction of metal fires [10].

The fire-extinguishing property of intercalated graphite is made possible by the ability of intercalated graphite to exfoliate upon contact with a fire. For example, a flame-retardant, flexible synthetic resin tube can be obtained from a composite of intercalated ("expandable") graphite and a polyolefinic resin can be used as a protective tube for electrical wires or cables [11].

2.3. Thermal insulators

Exfoliated graphite is commercially available as a thermal insulator, particularly one for molten metals [12]. As contact with a molten metal provides enough heat for exfoliation, intercalated graphite (not exfoliated) is commercially available under the name "hot top compound" for use at the top of molten metals, where it exfoliates immediately.

2.4. Conductive resin composites

Conductive resin composites can be obtained by blending exfoliated graphite and a thermoplastic resin. In this process, graphite flakes are exfoliated about 200 times in the direction of the c axis, and then ground. The ground exfoliated graphite and other ingredients are mixed and extruded into rods having an electrical resistivity of $3.5 \times 10^4\,\Omega$cm and a specific gravity of 1.29, compared with $5.5 \times 10^5\,\Omega$cm and 1.57, respectively, for a control containing carbon black instead of exfoliated graphite [13].

2.5. Electrodes

Electrodes of exfoliated graphite have been shown to be superior to those of platinum or ordinary graphite

0022–2461/87 $03.00 + .12 © *1987 Chapman and Hall Ltd.*

for electrolytic polymerization because platinum or ordinary graphite electrodes tend to be coated by the resulting polymer [14].

2.6. Protective layers on carbon crucibles

The service life of a carbon crucible for the melting of metals (e.g. aluminium) in vapour deposition can be increased by protecting it with a layer of exfoliated graphite [15].

2.7. Lubricant supports

Exfoliated graphite can serve as a support for a liquid or solid lubricant which is located in its pores. The advantages are that the material can be more conveniently handled than are conventional greases and that it does not lose its content of absorbed lubricant by liquefaction or collapse when the temperature is raised to the volatilization temperature of the absorbate [13]. An example is a paste formed by mixing 200 g of Mobil SHC lubricating oil (b.p. $< 170°$ C) and 10 g of exfoliated graphite; the paste is stable up to 250° C [16].

2.8. Battlefield obscurants

Due to its low density (about 0.004 g cm^{-3}), exfoliated graphite particles of 10 to 35 μm size, when dispersed in air, remain suspended for a long time. Furthermore, graphite is an effective absorber over a wide range of the electromagnetic spectrum from the ultraviolet to the microwave region. As a result, exfoliated graphite is being investigated by the US Army for use as a battlefield obscurant [17].

2.9. Moulded graphite products

Mouldable graphite is attractive technologically for the production of graphite articles. Moulded graphite products having a density of ~ 1.5 g cm^{-3} can be made by feeding exfoliated graphite from a hopper into a screw installed inside a cylinder, extruding by rotating the screw, feeding into a slit inside a mould and compressing [18].

2.10. Chemical reagents

Exfoliated graphite can serve as a chemical reagent of which the chemical reactivity is different from that of natural graphite. For example [19], in the reaction of exfoliated graphite, in comparison with natural graphite, with F_2 at 335 to 400° C, mainly $(C_2F)_n$ was obtained rather than $(CF)_n$. With exfoliated graphite, the reaction was complete in 10 h at 400° C or 80 h at 335° C; over 100 h at 400° C was needed for natural graphite.

2.11. Adsorption substrates

Exfoliated graphite can serve as a substrate for the study of adsorbed films because of its large surface area. Exfoliated graphite foil (i.e. flexible graphite, such as Grafoil of Union Carbide Corporation) is attractive for its N_2 surface area of 20 m^2 g^{-1}, but its mosaic spread is $\sim 7°$ full-width-half-maximum (FWHM) [20]. Exfoliated highly oriented pyrolytic graphite (HOPG) has an N_2 surface area of 4 m^2 g^{-1}, but its mosaic spread is only $\sim 2.2°$ FWHM [20]. Exfoliated single-crystal graphite flakes are furthermore attractive for probing orientational information in the layer planes [21].

Exfoliated graphite can be used as an adsorbent for gas chromatography for separating geometrical and structural isomers. Its gas chromatographic properties are close to those of graphitized thermal carbon black [22].

3. Types of exfoliation

Although all of the applications mentioned in the last section pertain to irreversibly exfoliated graphite, exfoliation can be either reversible or irreversible. The reversibility is a consequence of the fact that exfoliation is a phase transition.

3.1. Reversible exfoliation

Reversible exfoliation of graphite was first reported by Martin and Brocklehurst [23] on desorbed graphite–bromine based on pyrolytic graphite. They observed that (i) first exfoliation occurred at $\sim 170°$ C upon first heating, (ii) subsequent exfoliation occurred at $\sim 120°$ C in subsequent heating cycles, (iii) collapse occurred at $\sim 110°$ C upon cooling, (iv) second and subsequent exfoliation cycles were reversible, and (v) the expansion was up to 380% at 500° C.

Observations (i) to (iv) were repeatedly confirmed by other workers on pyrocarbon (HTT 3000° C) [24], HOPG [25] and single-crystal graphite [26], except that there were some differences in the transition temperatures among these graphite materials. In particular, definite differences exist between HOPG and single-crystal graphite, both of which were intercalated with bromine, desorbed and tested in the same way, and shown in Fig. 1 [26]:

1. The fractional expansion in the first exfoliation was larger in single-crystal graphite than in HOPG. For example, the fractional expansion at 300° C during the first cycle was 31 (or 3100%) for the single-crystal graphite and 24 for HOPG.
2. The collapse temperature was $210 \pm 10°$ C for single-crystal graphite and $100 \pm 10°$ C for HOPG. As a result, the hysteresis was relatively small between the collapse and the next expansion for single-crystal graphite.
3. For HOPG, a single exfoliation event consisted of multiple expansion spurts [25], whereas for single-crystal graphite the spurts (which appear as shoulders in the expansion against temperature curve) are absent.

Comparison of [23] and [25] shows that the fractional expansion increases sharply with increasing degree of crystallite orientation. [26] shows that an increase of the grain size has much less influence on the fractional expansion.

The fractional expansion also depends on the cycle number. For a graphite–bromine HOPG sample which had been desorbed prior to first exfoliation, the expansion in the second cycle was higher than that of the first cycle [25].

Exfoliation is accompanied by intercalate desorption, even if the sample has been desorbed prior to heating. The largest amount of desorption occurs

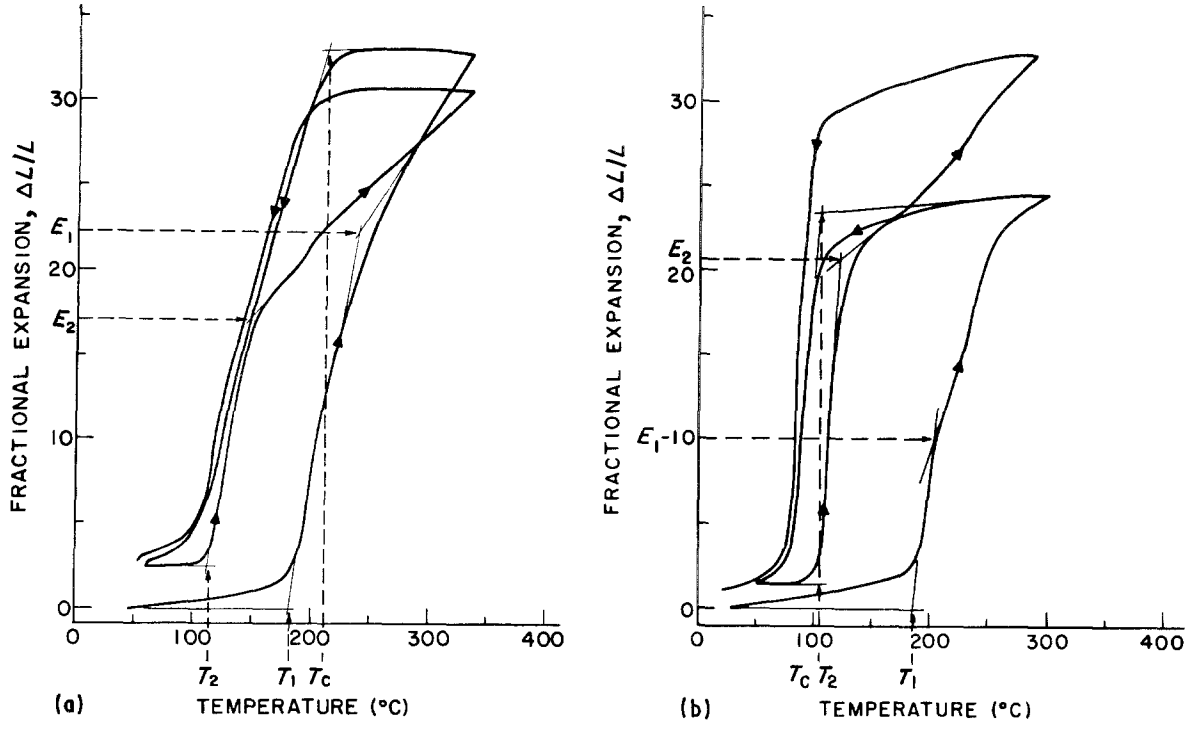

Figure 1 Fractional expansion against temperature during the first two exfoliation–collapse cycles of graphite–bromine based on (a) single-crystal graphite and (b) HOPG.

during the first two cycles. The amount of remaining bromine intercalate in subsequent cycles varies with $N^{1/2}$ where N is the number of exfoliation cycles. This suggests that the desorption is a diffusion process with an exfoliation cycle being analogous to a unit of desorption time [25].

3.2. Irreversible exfoliation

Irreversible exfoliation was first reported by Aylsworth in 1916 [27]. It requires temperatures higher than those necessary for reversible exfoliation. Ubbelohde [28] observed an irreversible expansion of ~ 10 at 350° C for graphite–bromine based on well-oriented graphite. The transition from reversible exfoliation to irreversible exfoliation is gradual. With exfoliation cycles to higher temperatures or longer times, the amount of residual expansion after the collapse on cooling increases until no second exfoliation occurs on reheating [25].

Irreversibly exfoliated graphite is generally more expanded than reversibly exfoliated graphite because of the higher temperatures used in irreversible exfoliation. Irreversible expansions as high as 300 are commonly used in technology.

4. Methods of exfoliation

Since true exfoliation is a phase transition which occurs at a well-defined elevated temperature, heating is necessary for it to occur. This heating can be achieved externally or internally.

4.1. Exfoliation by external heating

The most conventional heating source is a flame, through which the intercalated graphite is transported. The flame provides rapid heating to high temperatures. The flame temperature can be $\geqslant 1200°$ C [29], though lower temperatures such as 700 to 800° C are also possible [30]. The flame is located in a furnace which may be lined with SiO_2–Al_2O_3 materials to increase the service life [29]. Resistance and induction heating methods are also possible. More recently, infrared, microwave and laser heating methods have also been used [31]. For example, exfoliation was carried out by the passage of a 1 mm thick layer of a graphite intercalation compound on a conveyer belt through an infrared heating zone at a speed of $0.5\,m\,sec^{-1}$, a flux density of $800\,kW\,m^{-2}$ and a residence time of 0.4 sec [31].

Exfoliation is negligible when the graphite particle size is too small. The minimum particle size is about 75 μm [30]. Exfoliation is also negligible when the c axis stack height L_c is less than 75 nm [32].

Graphite must be intercalated before it can be exfoliated. In principle, any intercalate can be used. The most common choice of intercalation compound is graphite bisulphate obtained by reaction with a mixture of sulphuric and nitric acids, such as a 4 : 1 mixture of concentrated sulphuric acid and nitric acid (65%) [30] or a 3 : 1 mixture of concentrated sulphuric acid and nitric acid [33], because of its ability to yield expansions as high as 300. However, another intercalation compound that can also yield an expansion of 300 is $C_{24}K(THF)_2$, which is a ternary compound with potassium and tetrahydrofuran (THF) as intercalates [34, 35].

4.2. Exfoliation by internal heating

Exfoliation can also be achieved by internal heating, such as that obtained by passing an electric current through the intercalated graphite [36]. This method has recently been applied by passing a current along the c axis of graphite–bromine based on HOPG [36] and along a graphite fibre intercalated with iodine monochloride [37].

4.3. Expansion by excessive electrolytic intercalation

Expansion that results in the appearance of exfoliation can be achieved by excessive electrolytic intercalation [38]. For example, expansions exceeding 400 times have been obtained by excessive electrolytic intercalation of sulphuric acid in graphite at room temperature [38]. However, this expansion is scientifically different from true exfoliation, as it is not a phase transition.

5. Exfoliation of carbon fibres

The exfoliation of carbon fibres was not reported until 1983 [26] because it requires carbon fibres that are highly graphitic. Exfoliation not only expands the fibres, it also modifies the shape, morphology and surface texture of the fibres and lowers the density. Carbon fibres with C-shaped cross-sections, corrugated surfaces and a partially fibrillated structure were obtained by the exfoliation of Union Carbide Thornel P-100-4 pitch-based carbon fibres that had been intercalated with ICl [26, 37]. A larger expansion (up to ~ 150 times) was obtained by the exfoliation of benzene-derived graphite fibres that had been intercalated with $SbCl_5$, but the expansion was not uniform and caused extensive fracture of the graphite layers [39].

6. Mechanism of exfoliation

The origin of exfoliation lies in the vaporization of the intercalate [23–25, 40–42]. This is evidenced by the observation of endothermic differential thermal analysis (DTA) [24, 43] and differential scanning calorimetry (DSC) [44] peaks at the exfoliation temperature and the ideal-gas-law behaviour of the expansion [41–43].

The temperature T of the DTA endotherm in the second exfoliation cycle ($T = 105°C$ at $P = 1$ atm) is affected by the pressure P such that $\log P$ is a linear function of $1/T$ [24]. The slope of the plot of $\log P$ against $1/T$ yielded the value of 17 kcal mol^{-1} (71 kJ mol^{-1}) for ΔH. This value is much higher than that for the vaporization of bulk liquid bromine (7.3 kcal mol^{-1} or 31 kJ mol^{-1}) [24]. The value for $\Delta S/R$ is 29 for exfoliation, as compared to the value of 18 for the vaporization of bulk liquid bromine [24]. This large entropy value for exfoliation led Mazieres *et al.* [24] to suggest in 1975 that the bromine evaporates from a state in which its degree of organization is greater than in the liquid state. In 1977, it was observed that the bromine intercalate undergoes in-plane melting reversibly at 100°C [45]. Thus the second exfoliation temperature is very close to the intercalate melting temperature, so that intercalate vaporization follows closely after intercalate melting during the second and subsequent cycles. This is consistent with the high entropy of second exfoliation. The entropy change of first exfoliation should be quite different from that of the second exfoliation because the first exfoliation temperature is considerably higher than the intercalate melting temperature, but this value has not been reported.

The DTA endotherm at the first exfoliation temperature was observed even in graphite–bromine which was formed by reintercalating irreversibly exfoliated graphite–bromine [43]. Thus the first vaporization occurs at the same temperature even when it is not accompanied by exfoliation.

Only about 1/8 of the intercalate vaporizes during exfoliation, as shown by the recent pressure–volume–temperature measurement during the exfoliation of graphite–bromine based on HOPG [42].

Martin and Brocklehurst [23] reported that, for graphite–bromine based on pyrolytic graphite, the stress needed to stop exfoliation increased linearly with increasing temperature. However, it has recently been shown for graphite–bromine based on HOPG that the stress needed to stop exfoliation increases abruptly at the exfoliation temperature in a non-linear fashion [46]. Thus, all observations are now consistent with the occurrence of a phase transition during exfoliation.

Martin and Brocklehurst [23] proposed a model in which gaseous bromine bubbles within the lamellar structure of the graphite crystal are considered to be analogous to Griffith cracks. Higashida and Kamada [47] analysed the stress distribution around pressurized penny-shaped cracks in graphite near a free surface and concluded that two fracture modes are available. One fracture mode is brittle fracture as a Griffith crack, i.e. the crack diameter increases when the tensile stress in the c direction exceeds the fracture strength. The other fracture mode is the buckling of the walls of the cracks; when large bending moments exist at the crack tip, the flat crack may open to form a bubble. Anderson and Chung [25] proposed that the latter fracture mode is responsible for the expansion observed in exfoliation. This mode is possible because of the ease with which the graphite layers undergo shear. The observation of acoustic emission well before exfoliation [25] suggests that the penny-shaped cracks propagate initially as Griffith cracks, with very little net expansion, then fracture by buckling to produce exfoliation.

It was suggested by Hooley [48] that certain structural defects seal the edges of the graphite planes together, thus creating small gas-tight pockets in which the bromine is trapped. The experimental results of Anderson and Chung [25] indicated that neither pre-existing nor induced defects can be the source of the penny-shaped cracks. They proposed that the intercalate islands suggested by Daumas and Herold [49] determine the size of the penny-shaped cracks [25]. Furthermore, the size of the intercalate islands is expected to be determined by the intercalating conditions. Indeed the amount of expansion was found to increase with decreasing intercalate activity during intercalation [25]. In accordance with nucleation theory, as the reactant activity increases, competition between nucleation sites increases and the subsequent microstructure is finer. Hence, as the intercalate activity is decreased by dilution or by heating, the intercalate island size is expected to increase. For a compound of a given concentration, increased island size means that exfoliation can occur more easily and to a greater extent [25]. As the intercalate islands have

a size distribution and the relatively large ones tend to form bubbles more easily than the others, not every island succeeds in evolving into a bubble [42]. Therefore, only graphite with a sufficiently large value of L_c ($\geqslant 75$ nm) can be exfoliated [32].

Olsen *et al.* [50] suggested that intercalate pockets are formed near grain boundaries. However, it was observed that graphite–bromine based on HOPG and single-crystal graphite exfoliated with comparable ease and to comparable extents [26]. Therefore, grain boundaries cannot play a dominant role in the mechanism of exfoliation.

From the average thickness of the bubble wall determined by X-ray diffraction and the result of the pressure–volume–temperature measurement during exfoliation, it was deduced that, during exfoliation, the intercalate migrated laterally and formed aggregates which were at least 8 monolayers thick on the average [42]. The mechanism for the intercalate migration and aggregation is presently not clear.

Hooley [48] suggested the existence of gas-tight pockets in which the intercalate is trapped. However, if the intercalate mobility and solubility are high, the intercalate species may diffuse out of the gas bubbles and into the matrix in a short time in comparison with the length of time required for the exfoliation cycle [25]. For exfoliation at normal pressures, the loss of intercalate from the gas bubbles may even result in the collapse of the exfoliated structure. Subsequent heating and cooling will then cause negligible expansion. Such collapse during heating in the first exfoliation cycle was observed in graphite–nitric acid [25]. When diffusion is slower, as in the case of bromine, long periods of time and high temperature are necessary before appreciable collapse occurs [25].

Diffusion of the intercalate out of the sample through the matrix is one mechanism for the loss of excess intercalate. However, the gas cells themselves may serve as sinks for the excess intercalate. Under such circumstances, the matrix would lose intercalate while the sample as a whole would not. On subsequent exfoliation cycles, the enriched cells should expand to a greater degree. The latter possibility is consistent with the observation of a larger expansion during the second exfoliation than the first exfoliation for samples which are initially desorbed [25]. Yet another mechanism of intercalate loss is the bursting of the gas bubbles or the bubbles forming an interconnected network which in turn opens to the outside of the sample. Such violence may occur in the first couple of exfoliation cycles when the intercalate concentration is relatively high [25].

For certain intercalates, the origin of exfoliation is the thermal decomposition of the intercalate into a gas phase and another solid phase. Although it is not the vaporization of a single phase, it is a phase transition which yields a gaseous product, so the basic mechanism is still similar to what is mentioned above. An example of such a form of exfoliation is in the exfoliation of graphite–ferric chloride, where the overall reaction is in the form

$$FeCl_2(s) \rightarrow Cl_2(g) + Fe(s)$$

The escape of the chlorine sends the reaction to the right [51].

7. Structure of exfoliated graphite

Exfoliated graphite exhibits a honeycomb microstructure because of the gas bubbles, as revealed by scanning electron microscopy (SEM) [41, 51]. Fig. 2 is an SEM photograph showing this morphology. The bubble wall thickness is of the order of 50 nm [41, 42]. Each bubble contains a three-dimensional aggregate of at least 8 intercalate monolayers [42].

X-ray diffraction showed that irreversibly exfoliated pyrolytic graphite with a fractional expansion of 10 exhibits the same high degree of orientation as the parent material [50]. After the reversible exfoliation of single-crystal graphite–bromine, the in-plane unit cell and the twinned domain structure of the intercalate were found by X-ray diffraction to be preserved [26]. The in-plane superlattice ordering was observed even in irreversibly exfoliated graphite–bromine that had been heated for 1 h at 1700° C [25]. Thus, even highly expanded and irreversibly exfoliated graphite is truly intercalated, in spite of the low intercalate concentration.

The surface area of exfoliated graphite varies from intercalate to intercalate. For example, nitric acid is an intercalate which leads to considerable bursting of the gas bubbles whereas bromine is an intercalate which does not. As a result, nitric acid yields an exfoliated graphite with a much higher surface area than exfoliated graphite–bromine. However, even for nitric acid, the N_2 surface area is just $4\,m^2\,g^{-1}$ [20].

8. Transport properties

The transport properties are considered after irreversible exfoliation, during reversible exfoliation and when exfoliation is suppressed.

8.1. Properties after irreversible exfoliation

8.1.1. Electrical resistivity

The *a* axis electrical resistivity of irreversibly exfoliated pyrolytic graphite bisulphate at 300 K is $2 \times 10^{-4}\,\Omega$cm when the fractional expansion is 2.8, as compared with the value of $5 \times 10^{-5}\,\Omega$cm prior to exfoliation [50]. The *a* axis electrical resistivity of

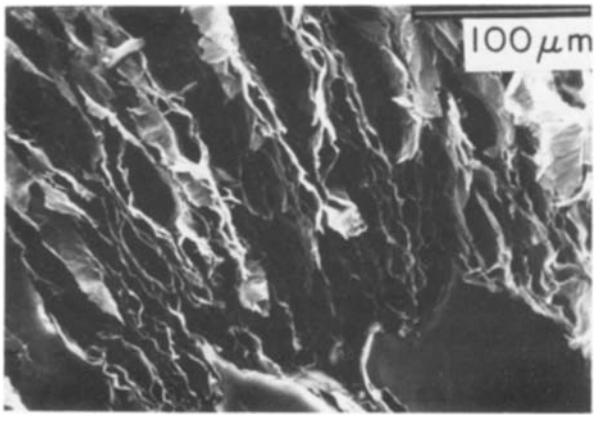

Figure 2 SEM photograph of the fracture surface of an exfoliated graphite–polyester composite, showing the honeycomb microstructure of the exfoliated graphite.

irreversibly exfoliated HOPG graphite–bromine at room temperature is $5.4 \times 10^{-4}\,\Omega$cm, as compared with the value of $2.4 \times 10^{-6}\,\Omega$cm prior to exfoliation [52]. Hence, exfoliation increases the *a* axis resistivity due to the bending of the graphite layers.

The *c* axis electrical resistivity of irreversibly exfoliated pyrolytic graphite bisulphate at 300 K is $0.11\,\Omega$cm when the fractional expansion is 2.8, as compared with the value of $0.22\,\Omega$cm prior to exfoliation [50]. The *c* axis electrical resistivity of irreversibly exfoliated HOPG graphite–bromine at room temperature is $3.0 \times 10^{-2}\,\Omega$cm, as compared with the value of $6.3 \times 10^{-1}\,\Omega$cm prior to exfoliation [52]. Hence, exfoliation decreases the *c* axis electrical resistivity due to the *c* axis conduction path made possible by the bending of the graphite layers.

The *c* axis electrical resistivity of irreversibly exfoliated pyrolytic graphite bisulphate decreases with increasing temperature from 300 to 800 K both before and after exfoliation [50].

The *a* axis electrical resistivity of irreversibly exfoliated HOPG (UCAR-ZYX graphite) is $8.16 \times 10^{-4}\,\Omega$cm at 300 K and it decreases with increasing temperature from 25 to 300 K [53]. However, it increases with increasing temperature from 1.5 to 25 K [53]. This unusual temperature dependence was explained by considering two conduction mechanisms acting in parallel: an ordinary metallic one at low temperatures and a hopping-like one with (temperature) exponent 1/4 which extends up to about the liquid-nitrogen temperature range. The localized levels are tentatively associated with dislocations which bound stacking-fault ribbons [53].

8.1.2. Thermoelectric power

The *a* axis thermoelectric power of irreversibly exfoliated pyrolytic graphite bisulphate at 325 K is $-8\,\mu V\,K^{-1}$ when the fractional expansion is 2.8, as compared with the value of $-7\,\mu V\,K^{-1}$ prior to exfoliation [50]. The *a* axis thermoelectric power decreases linearly with increasing temperature from 325 to about 600 K in the same manner both before and after exfoliation [50].

The *c* axis thermoelectric power of irreversibly exfoliated pyrolytic graphite bisulphate at 315 K is $-5\,\mu V\,K^{-1}$ when the fractional expansion is 2.7, as compared with the value of $+2\,\mu V\,K^{-1}$ prior to exfoliation [50]. The *c* axis thermoelectric power after exfoliation increases very slightly with increasing temperature from 425 to 700 K; before exfoliation it increases significantly with increasing temperature from 320 to 665 K [50].

The *a* axis thermoelectric power of irreversibly exfoliated HOPG (UCAR-ZYX graphite) is $+9\,\mu V\,K^{-1}$ at 300 K, as compared with the value of $-7\,\mu V\,K^{-1}$ prior to exfoliation [54]. Hence, there is discrepancy between the values of the *a* axis thermoelectric power of irreversibly exfoliated graphite in [50] and [54]. The *a* axis thermoelectric power of irreversibly exfoliated HOPG increases significantly with increasing temperature from 30 to 220 K, but decreases significantly with increasing temperature from 1.7 to 30 K and decreases slightly with increasing temperature from 220 to 290 K [54]. For HOPG (without intercalation or exfoliation), the *a* axis thermoelectric power increases significantly with increasing temperature from 30 to 140 K, but decreases significantly with increasing temperature from 1.7 to 30 K and from 140 to 300 K [54]. Hence, a large negative anomaly due to phonon drag occurs at around 30 K both before and after exfoliation. However, at higher temperatures up to 300 K, the thermoelectric power is more positive after exfoliation than before intercalation, probably due to a small acceptor-like residue in the material after exfoliation [54]. The thermoelectric power after exfoliation has been tentatively separated into its diffusion and phonon-drag components [54].

8.1.3. Thermal conductivity

The *a* axis thermal conductivity of irreversibly exfoliated pyrolytic graphite bisulphate at 300 K is $4\,W\,cm^{-1}\,K^{-1}$ when the fractional expansion is 3.1, as compared with the value of $13\,W\,cm^{-1}\,K^{-1}$ prior to exfoliation [50]. Hence exfoliation decreases the *a* axis thermal conductivity due to the bending of the graphite layers and the increased phonon–phonon scattering. The conductivity decreases slightly with increasing temperature from 300 to 400 K both before and after exfoliation [50].

The *c* axis thermal conductivity of irreversibly exfoliated pyrolytic graphite bisulphate at 350 K is $0.03\,W\,cm^{-1}\,K^{-1}$ when the fractional expansion is 3, as compared with the value of $0.65\,W\,cm^{-1}\,K^{-1}$ before exfoliation [50]. Hence exfoliation decreases the *c*-axis thermal conductivity due to the decrease in density.

Since exfoliation decreases the thermal conductivity along both the *a* axis and the *c* axis, exfoliated graphite is a valuable thermal insulator material.

8.2. Properties during reversible exfoliation

The *c* axis electrical resistivity is the only transport property that has been measured *in situ* during reversible exfoliation. The measurement was made on HOPG graphite–bromine. The resistivity was found to decrease abruptly at the exfoliation temperature during reversible exfoliation [52]. Although the *c* axis electrical resistivity varies much with temperature, the *c* axis electrical resistance is quite independent of temperature because the elongation of the sample along the *c* axis occurs while the *c* axis electrical resistivity decreases [52].

8.3. Properties when exfoliation is suppressed

Even when exfoliation is suppressed, either by an externally applied mechanical force or internal microstructural hindrance, the transport properties are affected. This is because the transport properties are sensitive to microscopic structural changes, such as a minute bending of the graphite layers, even in the absence of a macroscopic expansion.

8.3.1. Suppression by an externally applied mechanical force

The *c* axis electrical resistivity of HOPG graphite–bromine increases and then decreases upon heating

and increases and then decreases upon subsequent cooling, when the graphite–bromine sample is under mechanical constraint from expansion along the *c* axis [36]. Note that this effect is smaller and totally different from that of Section 8.2. It is attributed to the initiation of intercalate bubble formation as the sample is heated. This effect must be considered in the use of intercalated graphite as an electrical conductor.

8.3.2. Suppression by internal microstructural hindrance

Exfoliation requires a graphitic material with good alignment of the carbon layers, as mentioned in Section 3.1. An intercalated graphite based on a relatively poor graphite material might not be able to exfoliate due to internal microstructural hindrance, but the effect on the electrical resistivity might still be present.

Miyauchi *et al.* [55] observed that the *a* axis electrical resistivity of graphite–bromine based on artificial graphite heat-treated at 3000° C increased with increasing temperature up to 800° C and subsequently decreased with decreasing temperature under no mechanical constraint and in the absence of exfoliation. The increase in resistivity began at about 200° C upon heating; the decrease in resistivity began at about 320° C upon cooling [55]. The origin of this change in the *a* axis resistivity is attributed to the initiation of intercalate bubble formation, which disturbs the planar nature of the graphite layers and thus increases the *a* axis electrical resistivity [36]. The relatively high transition temperatures observed by Miyauchi *et al.* [55] is due to the fact that their graphite material was not well oriented like HOPG. The X-ray diffraction, thermal diffusivity and heat capacity results of Miyauchi and Takahashi [56] are consistent with the above-mentioned interpretation. An effect of a similar origin also occurs in the *a* axis magnetic susceptibility [57].

Most carbon fibres have a degree of crystalline perfection and alignment which is not sufficient for exfoliation, so exfoliation is suppressed by internal microstructural hindrance in most carbon fibres and exfoliation requires exceptionally high temperatures. However, the electrical resistivity of the fibres can still be affected in the absence of exfoliation. The electrical resistance (*a* axis) of graphite–ICl pitch-based carbon fibres (Union Carbide Thornel P-100-4) was found to increase quite abruptly and reversibly over a temperature range which is below that for the exfoliation of these fibres [58]. This effect might again be due to the initiation of intercalate bubble formation.

9. Mechanical properties

Irreversibly exfoliated graphite is mechanically weak. No measurement of its mechanical properties has been reported. The only report is in the compressive mechanical property of reversibly exfoliated graphite at various temperatures that are sufficient for exfoliation [42]. The compressive Young's modulus of reversibly exfoliated graphite at 180 to 200° C is about 1.4 MPa [42].

10. Graphite foils

Flexible graphite foils can be formed by rolling an aggregate of irreversibly exfoliated graphite flakes without a binder [5], because of the ability of the exfoliated graphite flakes to be mechanically interlocked. They are now manufactured all over the world for use as gaskets and seals (Section 2.1) because of their flexibility, lubricity and temperature resistance.

10.1. Formation of graphite foils

The process of producing graphite foils comprises compressing or compacting, under a predetermined load and in the absence of a binder, exfoliated graphite particles (known as worms because of their appearance) which have a *c*-direction dimension that is at least 80 times and preferably 200 times that of the original particles so as to form a substantially flat, flexible, integrated graphite foil [1]. The exfoliated graphite particles once compressed will maintain the compression set [1].

The industrial process involves depositing a predetermined height of the exfoliated graphite particles continuously on to a travelling surface of substantial width and passing the mass through a pair of superposed rollers; the spacing provided between the rollers is sufficient to compress or compact the exfoliated graphite into a coherent, self-sustaining long flat sheet, which is then passed through another pair of superposed rollers, the spacing between which has been adjusted to further compress the sheet [1]. An alternative but not continuous process involves simply compression at 100 kg cm^{-2} [35].

10.2. Properties of graphite foils

The density of a graphite foil can range from 0.05 to 2.2 g cm^{-3} [1, 59]. The specific surface area increases with decreasing density; for a density of 0.05 g cm^{-3}, it is 38.2 m^2 g^{-1} [59].

The compressive modulus ranges from 0.18 to 0.37 GPa. The plot of compressive stress against strain normal to the foil plane is concave to the stress axis. The restoring force in compression is too large to be attributed to the trapping of gas in the pores of the foil. It is attributed to the spring-like action of graphite basal plane segments tilted out of the plane of the foil. Irreversible work expended in compressing isolated exfoliated graphite flakes to foil, 5 to 10 J g^{-1}, is accompanied by reduction of the surface area to approximately two-thirds of its original value [59].

The tensile strength is 6 MPa for a density of 1.10 g cm^{-3} [59]. It increases with increasing density [1] and is less than observed in bulk graphites, but values of the work of extension to fracture, 10 to 60 mJ g^{-1}, are comparable [59]. The tensile modulus also increases with increasing density [1]; typical values range from 0.5 to 3.0 GPa [59]. The tensile behaviour of graphite foils is attributed to the mechanical linkage of asperities on adjacent exfoliated graphite flakes as they are compressed [59].

The electrical resistivity of graphite foils at 300 K is 1.1×10^{-3} Ω cm in the foil plane [1, 35, 53] and 1.15×10^{-1} Ω cm perpendicular to the foil plane for a density of 0.82 g cm^{-3} [53]. The resistivity in the foil

plane decreases with increasing density, whereas that perpendicular to the foil plane increases with increasing density [53]. Hence, the anisotropy increases with increasing density, as compression causes the alignment of the graphite layers. The temperature dependence of the resistivity in either direction in the temperature range 1.5 to 300 K shows a metallic-like behaviour below 25 K and an activated character at high temperatures [53]; this behaviour is the same as that of the exfoliated graphite in the foil plane (*a* axis) prior to compression (Section 8.1.1.).

The thermoelectric power of graphite foils at 300 K is $+5\,\mu V\,K^{-1}$ in the foil plane and $+1\,\mu V\,K^{-1}$ perpendicular to the foil plane for a density of $0.82\,g\,cm^{-3}$ [54]. The thermoelectric power in the foil plane decreases with increasing density, whereas that perpendicular to the foil plane increases with increasing density [54]. The temperature dependence in either direction in the temperature range 1.7 to 300 K shows a large negative anomaly similar to that of HOPG at around 30 K [53]; this behaviour is also similar to that of exfoliated graphite in the foil plane (*a* axis) prior to compression (Section 8.1.2.).

The heat capacity C_p of graphite foils at 310 to 650 K is higher than that of the untreated (pristine) graphite. This is attributed to the less perfect structure of the graphite foils [60]. However it might be due to the presence of the residual intercalate in graphite foils.

Graphite foils of density less than 1.1 to $1.5\,g\,cm^{-3}$ exhibit residual elongation after heating to 1200 K and subsequent cooling, whereas those of higher density are destroyed upon heating to 650 K [60]. This effect is attributed to the pyrolysis of the graphite [60], but the suddenness of the destruction suggests that it may be due to re-exfoliation. It was concluded that the thermal stability of the graphite foils decreases with increasing density [60].

11. Composites

Composites comprising exfoliated graphite were first reported in 1915 by Alysworth [61], who combined irreversibly exfoliated graphite with a thermosetting binder. The use of a thermoplastic binder is also possible [13]. Recently, oriented composites of exfoliated graphite and a polyimide have been prepared by hot-pressing a mixture of intercalated graphite flakes and the resin at 200° C and 47 kPa, so that exfoliation and curing occur in one step [62]. These oriented composites exhibit superior flexural properties [62]. Composites (not oriented) of irreversibly exfoliated graphite in high-density polyethylene have also recently been made [63]. Their dielectric constant correlates with the *in situ* volumetric fraction of compressible exfoliated filler particles; it ranges from 2.23 to 125. The minimum electrical resistivity of the composites is $0.1\,\Omega\,cm$ at a graphite content of 40 vol % [63]. This recent rise in interest in such composites is related to the need for low-density mouldable materials for electromagnetic interference (EMI) shielding.

Composites of irreversibly exfoliated graphite in furan resins have been found to be useful as gaskets with low adhesion to the pressing plates [7]. A composite of exfoliated graphite and fibre fillers in a rubber binder has been found to be useful as a packing material with a high sealing strength even under repeated heating cycles [9]. Furthermore, a refractory sealing material has been obtained by adding a binder and an expandable graphite to a refractory aggregate and then heating [8].

12. Exfoliation of coke

Coke which has been graphitized at 2800° C, intercalated with potassium and THF, and then heated at 800° C exfoliates to an expansion of about 20 times [35]. The use of concentrated acids instead of potassium and THF does not yield exfoliation [35]. This is attributed to the exceptional tendency for potassium intercalation in materials that are not very graphitic. Indeed the possibility of intercalating coke with potassium has been demonstrated [64].

13. Summary

This paper is the first review paper on the exfoliation of graphite. It covers scientific and technological developments in this subject since its inception in 1915. However, most of the progress occurred after 1968, when flexible graphite foils made from exfoliated graphite were invented for use as gaskets and seals. Most of the scientific work was on the mechanism of exfoliation and the transport properties. The recent impetus in this field is due to the attraction of exfoliated graphite composites for electromagnetic interference shielding and the invention of exfoliated carbon fibres in 1983.

References

1. J. H. SHANE, R. J. RUSSELL and R. A. BOCHMAN, US Patent 3 404 061 (1968).
2. Z. HUANG, Runhua Yu Mifeng Vol. 6 (1981) pp. 28–32.
3. L. SHI and Y. FAN, Runhua Yu Mifeng Vol. 27 (1981) pp. 17–24, 70.
4. R. K. FLITNEY, *Tribology Int.* **19** (1986) 181.
5. T and N Materials Research Ltd, Jpn. Kokai Tokkyo Koho JP 57 168 978 (1982).
6. Nippon Pillar Packing Co. Ltd, Jpn. Kokai Tokkyo Koho JP 58 124 863 (1983).
7. A. HIRSCHVOGEL, Ger. Offen. DE 3 244 595 (1984).
8. Nippon Steel Corp., Jpn. Kokai Tokkyo Koho JP 57 164 279 (1982).
9. Nippon Pillar Packing Co. Ltd, Jpn. Kokai Tokkyo JP 59 68 387 (1984).
10. Cesa SA, UK Patent 1 588 876 (1981).
11. Furukawa Electric Co., Jpn. Kokai Tokkyo Koho JP 58 17 284 (1983).
12. H. MIKAMI, Jpn. Kokai Tokkyo Koho JP 76 96 793 (1976).
13. Mitsui Toatsu Chemicals, Inc., Jpn. Kokai Tokkyo Koho JP 59 81 349 (1984).
14. Kao Corp., Jpn. Kokai Tokkyo Koho JP 59 78 204 (1984).
15. Hitachi Chemical Co. Ltd, Jpn. Kokai Tokkyo Koho JP 58 58 278 (1983).
16. A. W. ATKINSON, UK Patent Application GB 2 128 629 (1984).
17. W. L. GARRETT, J. SHARMA, J. PINTO and H. PRASK, Report ARL CD-TR-81008, AD-E400 617 (National Technical Information Service of USA, 1981).
18. Fukubi Kagaku Kogyo KK, Jpn. Kokai Tokkyo Koho JP 57 49 367 (1982).
19. N. WATANABE, A. IZUMI and T. NAKAJIMA, *Kenkyu Hokoku-Asahi Garasu Kogyo Gijutsu Shoreikai* **39** (1981) 15.

20. M. B. DOWELL, Ext. Abstract Programme – Biennial Conference on Carbon, Vol. 13 (American Carbon Society, 1977) pp. 136, 137.
21. R. CLARKE, P. M. HORN, S. E. NAGLER and T. F. ROSENBAUM, *J. Appl. Phys.* **55** (1984) 1231.
22. N. N. ARGUL', N. V. KOVALEVA, I. L. MAR'YASIN and G. A. MISHINA, *Colloid J. USSR* **44** (1982) 274.
23. W. H. MARTIN and J. E. BROCKLEHURST, *Carbon* **1** (1964) 133.
24. C. MAZIERES, G. COLIN, J. JEGOUDEZ and R. SETTON, *ibid.* **13** (1975) 289.
25. S. H. ANDERSON and D. D. L. CHUNG, *ibid.* **22** (1984) 253.
26. *Idem, Synth. Met.* **8** (1983) 343.
27. J. W. AYLESWORTH, US Patent 1 191 383 (1916).
28. A. R. UBBELOHDE, *Br. Coal Util. Res. Assoc. Gaz.* **51** (1964) 1.
29. Hitachi Chemical Co. Ltd, Jpn. Kokai Tokkyo Koho JP 59 69 413 (1984).
30. B. FINDEISEN and M. THOMASIUS, Ger. (East) DD 150 739 (1981).
31. A. HIRSCHVOGEL and H. ZIMMERMANN, European Patent Application EP 87 489 (1983).
32. M. B. DOWELL, Ext. Abstract Programme – Biennial Conferences on Carbon, Vol. 12 (American Carbon Society, 1975) pp. 31, 32.
33. S. F. McKAY, *J. Appl. Phys.* **35** (1964) 1992.
34. M. INAGAKI and Toyo Carbon Co. Ltd, Jpn. Kokai Tokkyo Koho JP 58 156 515 (1983).
35. M. INAGAKI, K. MURAMATSU, Y. MAEDA and K. MAEKAWA, *Synth. Met.* **8** (1983) 335.
36. D. D. L. CHUNG and LAN W. WONG, *Carbon* **24** (1986) 639.
37. S. H. ANDERSON and D. D. L. CHUNG, *ibid.* **22** (1984) 613.
38. Z. XU and X. MO, Ext. Abstract Programme – Biennial Conferences on Carbon, Vol. 17 (American Carbon Society, 1985) pp. 59, 60.
39. H. JIMENEZ-GONZALEZ, J. S. SPECK, G. ROTH, M. S. DRESSELHAUS and M. ENDO, *Carbon* **24** (1986) 627.
40. K. AOKI, T. HIRAI and S. YAJIMA, *J. Mater. Sci.* **6** (1971) 140.
41. M. B. DOWELL, Ext. Abstract Programme – Biennial Conference on Carbon, Vol. 12 (1975) p. 35.
42. D. D. L. CHUNG, *Carbon* **25** (1987) 361.
43. C. MAZIERES, G. COLIN, J. JEGOUDEZ and R. SETTON, *ibid.* **14** (1976) 176.
44. L. W. WONG and D. D. L. CHUNG, unpublished results (1986).
45. D. D. L. CHUNG, G. DRESSELHAUS and M. S. DRESSELHAUS, *Mater. Sci. Eng.* **31** (1977) 107.
46. D. D. L. CHUNG and L. W. WONG, *Int. J. Thermophys.* in press.
47. Y. HIGASHIDA and K. KAMADA, *J. Nucl. Mater.* **73** (1978) 30.
48. J. G. HOOLEY, *Nature* **190** (1961) 529.
49. N. DAUMAS and A. HEROLD, *CR Acad. Sci.* **C268** (1969) 373.
50. L. C. OLSEN, S. E. SEEMAN and H. W. SCOTT, *Carbon* **8** (1970) 85.
51. R. E. STEVENS, S. ROSS and S. P. WESSON, *ibid.* **11** (1973) 525.
52. D. D. L. CHUNG and L. W. WONG, *Synth. Met.* **12** (1985) 533.
53. C. UHUR and L. M. SANDER, *Phys. Rev.* **B27** (1983) 1326.
54. C. UHUR, *ibid.* **B25** (1982) 4167.
55. K. MIYAUCHI, Y. TAKAHASHI and T. MUKAIBO, *Carbon* **9** (1971) 807.
56. K. MIYAUCHI and Y. TAKAHASHI, *ibid.* **14** (1976) 35.
57. A. MARCHAND and P. ESPELETTE, Ext. Abstract Programme – Biennial Conference of Carbon, Vol. 17 (American Carbon Society, 1985) pp. 67, 68.
58. D. D. L. CHUNG and LAN W. WONG, *Carbon* **24** (1986) 443.
59. M. B. DOWELL and R. A. HOWARD, *ibid.* **24** (1986) 311.
60. S. A. ALFER, A. S. SKOROPANOV, A. A. VECHER, L. S. MALEI and M. D. MALEI, *Thermochim. Acta* **88** (1985) 489.
61. J. W. ALYSWORTH, US Patent 1 137 373 (1915).
62. L. W. WONG and D. D. L. CHUNG, in Proceedings of 18th International SAMPE Technical Conference, Covina, California, 1986, pp. 114–123.
63. Y. S. WANG, M. A. O'GURKIS and J. T. LINDT, *Polym. Compos.* **7** (1986) 349.
64. D. BERGER, B. CARTON, A. METROT and A. HEROLD, in "Chemistry and Physics of Carbon", Vol. 12, edited by P. L. Walker Jr and P. A. Thrower (1975).

Received 1 May
and accepted 6 May 1987